Chiral Copper Hydrides

International Edition: DOI: 10.1002/anie.201506736
German Edition: DOI: 10.1002/ange.201506736

Diselenophosphate-Induced Conversion of an Achiral $[Cu_{20}H_{11}\{S_2P(OiPr)_2\}_9]$ into a Chiral $[Cu_{20}H_{11}\{Se_2P(OiPr)_2\}_9]$ Polyhydrido Nanocluster

*Rajendra S. Dhayal, Jian-Hong Liao, Xiaoping Wang, Yu-Chiao Liu, Ming-His Chiang, Samia Kahlal, Jean-Yves Saillard, and C. W. Liu**

Abstract: *A polyhydrido copper nanocluster, $[Cu_{20}H_{11}\{Se_2P(OiPr)_2\}_9]$ ($\mathbf{2_H}$), which exhibits an intrinsically chiral inorganic core of C_3 symmetry, was synthesized from achiral $[Cu_{20}H_{11}\{S_2P(OiPr)_2\}_9]$ ($\mathbf{1_H}$) of C_{3h} symmetry by a ligand-exchange method. The structure has a distorted cuboctahedral Cu_{13} core, two triangular faces of which are capped along the C_3 axis, one by a Cu_6 cupola and the other by a single Cu atom. The Cu_{20} framework is further stabilized by 9 diselenophosphate and 11 hydride ligands. The number of hydride, phosphorus, and selenium resonances and their splitting patterns in multinuclear NMR spectra of $\mathbf{2_H}$ indicate that the chiral $Cu_{20}H_{11}$ core retains its C_3 symmetry in solution. The 11 hydride ligands were located by neutron diffraction experiments and shown to be capping μ_3-H and interstitial μ_5-H ligands (in square-pyramidal and trigonal-bipyramidal cavities), as supported by DFT calculations on $[Cu_{20}H_{11}(Se_2PH_2)_9]$ ($\mathbf{2'_H}$) as a simplified model.*

Ligand replacement has become a subject of intense interest as it serves as a means to tune the surface structure of metal nanoparticles (NPs)[1] and thus their optical and electronic properties.[2] The situation becomes more interesting in the case of atomically precise gold nanoclusters.[3] For example, thiol-ligand exchange in molecularly pure $[Au_{38}(pet)_{24}]$ (pet = $^-S(CH_2)_2Ph$) with 4-*tert*-butylbenzenethio (tbbt) gave a new $[Au_{36}(tbbt)_{24}]$ nanocluster. Surprisingly, the intrinsically chiral $[Au_{38}(pet)_{24}]$ was transformed into achiral $[Au_{36}(tbbt)_{24}]$.[4] In parallel with this synthesis of thiolate-protected gold nanoclusters, recent studies have demonstrated that stable gold nanoclusters can be fabricated by the replacement of thiolate with selenolate ligands (^-SeR).[5] However, to the best of our knowledge, there have been no studies reported so far on the structure of ligand-supported, chiral polyhydrido metal nanoclusters generated by utilizing a ligand-exchange method.

Transition-metal hydrides found in solid-state and molecular forms[6] play extensive roles in both homogeneous and heterogeneous catalysis[7,8] and hydrogen-storage technology.[9] A binary copper hydride has been known since 1844,[10] and the first neutron-diffraction evidence of hexameric $[Cu_6H_6(PR_3)_6]$ copper hydrides,[11] also known as Stryker reagents, was pivotal for their development as catalysts for C–F bond activation,[12] reduction, and hydrogenation.[13] Copper hydride complexes generated in situ with chiral phosphine ligands have been used for the stereoselective conjugate reduction of a range of carbonyl compounds.[14] Clearly, the induction of chirality in any class of metal hydrides is of added value because of the importance of such chiral complexes for asymmetric catalysis.[15] Recently, the chemistry of copper hydride nanoclusters has been rapidly developed by several research groups.[16] This new research area has promising applications.[12,13] Following the synthesis and isolation of air- and moisture-stable copper(I) hydride clusters $[Cu_8(\mu_4\text{-}H)L_6]^+$ and $[Cu_7(\mu_4\text{-}H)L_6]$ stabilized by dichalcogen ligands (L),[17] we recently reported three symmetrical types of nanoscale copper(I) polyhydrido clusters, namely, $[Cu_{20}H_{11}L_9]$,[18] $[Cu_{28}H_{15}L_{12}]^+$,[19] and $[Cu_{32}H_{20}L_{12}]$,[20] with peculiar structural features and potential applications in solar H_2 evolution. We report herein the replacement of dithio- with diselenophosphate ligands by the treatment of a pure, nanospherical cluster, $[Cu_{20}H_{11}\{S_2P(OiPr)_2\}_9]$ ($\mathbf{1_H}$), with $NH_4[Se_2P(OiPr)_2]$ to afford $[Cu_{20}H_{11}\{Se_2P(OiPr)_2\}_9]$ ($\mathbf{2_H}$). The solid-state structure of $\mathbf{2_H}$, as elucidated by low-temperature X-ray diffraction (XRD), was supported by elemental analysis and multinuclear (^1H, ^2H, ^{77}Se, and ^{31}P) NMR spectroscopy. Neutron diffraction of $\mathbf{2_H}$ established the location of the hydride ligands, as supported by density functional theory (DFT) investigations on the simplified model $[Cu_{20}H_{11}(Se_2PH_2)_9]$ ($\mathbf{2'_H}$). Astonishingly, the structure of $\mathbf{2_H}$ was drastically different from that of the starting material $\mathbf{1_H}$ and revealed that an achiral molecule $\mathbf{1_H}$ of C_{3h} symmetry had been converted into an intrinsically chiral molecule $\mathbf{2_H}$ of C_3 symmetry. We also developed a direct synthetic route to produce $\mathbf{2_H}$ in moderate yield by a stoichiometric reaction of a copper(I) salt, $NH_4[Se_2P(OiPr)_2]$, and BH_4^-. The dichalcogen-stabilized polyhydrido copper(I)

[*] Dr. R. S. Dhayal, J.-H. Liao, Prof. C. W. Liu
Department of Chemistry, National Dong Hwa University
No. 1, Sec. 2, Da Hsueh Road, Shoufeng
Hualien 97401 (Taiwan R.O.C.)
E-mail: chenwei@mail.ndhu.edu.tw
Homepage: http://faculty.ndhu.edu.tw/~cwl/index.htm
Dr. R. S. Dhayal
Centre for Chemical Sciences, School of Basic and Applied Sciences
Central University of Punjab, Bathinda-151 001 (India)
Dr. S. Kahlal, Prof. J.-Y. Saillard
UMR-CNRS, 6226 "Institut des Sciences Chimiques de Rennes"
Université de Rennes 1, 35042 Rennes Cedex (France)
Dr. X. Wang
Chemical and Engineering Materials Division
Neutron Sciences Directorate, Oak Ridge National Laboratory
Oak Ridge 37831 (USA)
Dr. Y.-C. Liu, Dr. M.-H. Chiang
Institute of Chemistry, Academica Sinica, Taipei, 115 (Taiwan R.O.C.)

Supporting information for this article is available on the WWW under http://dx.doi.org/10.1002/anie.201506736.

nanoclusters $\mathbf{1_H}$ and $\mathbf{2_H}$ with their distinct molecular structures and metal cores have chemical formulas that differ only in the nature of the chalcogen (S vs. Se) and can therefore be considered as pseudoisomers.

Nanocluster $\mathbf{1_H}$ reacted with $NH_4[Se_2P(OiPr)_2]$ (12 equiv) at −35 °C in solution to yield $\mathbf{2_H}$ within 2 hours; this transformation could be monitored by ^{31}P NMR spectroscopy (see Figure S1 in the Supporting Information). In a direct synthetic approach, $\mathbf{2_H}$ was also synthesized in moderate yield by a one-pot reaction in the solvent THF (see the Supporting Information). Nanocluster $\mathbf{2_H}$ was moderately air- and moisture-stable in the solid state; in solution it decomposed gradually within a few days, but it was reasonably stable under an inert atmosphere. The molecular formula of $\mathbf{2_H}$ was established by electrospray ionization mass spectrometry (ESI-MS; Figure 1). ESI-MS (positive-ion mode) of $\mathbf{2_H}$ and $\mathbf{2_D}$ revealed a prominent peak at *m*/*z* 4042.8 (calcd: 4043.08) and *m*/*z* 4052.9 (calcd: 4053.8), which correspond to a formula of $[Cu_{20}H_{10}\{Se_2P(OiPr)_2\}_9]^+$ $[\mathbf{2_H}-H]^+$ and $[Cu_{20}D_{10}\{Se_2P(OiPr)_2\}_9]^+$ $[\mathbf{2_D}-D]^+$, respectively (Figure 1; see also Figure S2). Mass spectra also displayed the dicationic (2+) species $[Cu_{20}H_9\{Se_2P(OiPr)_2\}_9]^{2+}$ (*m*/*z* 2022.9; calcd: 2022.4) and $[Cu_{20}D_9\{Se_2P(OiPr)_2\}_9]^{2+}$ (*m*/*z* 2026.4; calcd: 2026.4). The theoretical isotopic patterns of the monocationic ($[\mathbf{2_H}-H]^+$, $[\mathbf{2_D}-D]^+$) and dicationic species ($[\mathbf{2_H}-2H]^{2+}$, $[\mathbf{2_D}-2D]^{2+}$) show great resemblance to the corresponding experimental patterns (see insets in Figure 1 and Figure S2). A 10.1 mass-unit difference between the $[\mathbf{2_H}-H]^+$ and $[\mathbf{2_D}-D]^+$ species confirmed the presence of 11 hydride ligands in the neutral $\mathbf{2_H}$ species.

The cluster $\mathbf{2_H}$ crystallizes as a racemate in the space group $R\bar{3}$. The solid-state molecular structure of the left-handed isomer, consisting of three anticlockwise copper strands of ideal C_3 symmetry, exhibits a fairly distorted, cuboctahedral

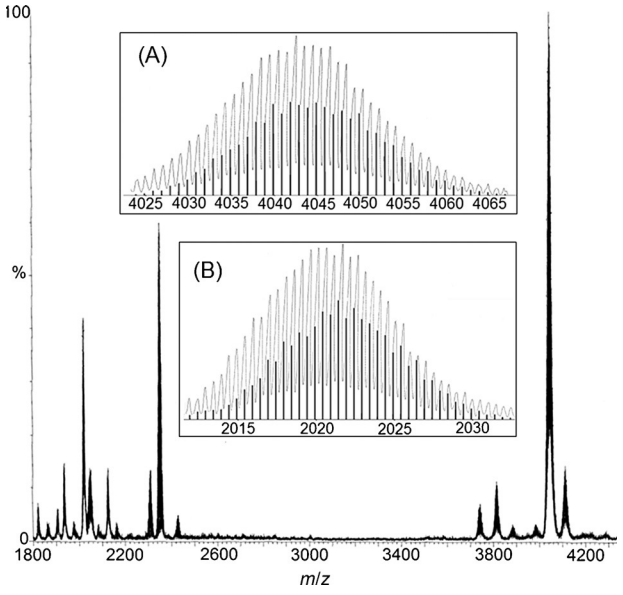

Figure 1. ESI-MS spectrum of $\mathbf{2_H}$. A,B) Experimental (top) and theoretical isotopic patterns (bottom) for $[Cu_{20}H_{10}\{Se_2P(OiPr)_2\}_9]^+$ (A) and $[Cu_{20}H_9\{Se_2P(OiPr)_2\}_9]^{2+}$ (B).

Cu_{13} core (Figure 2a). Whereas a regular Cu_{12} cuboctahedron can be described as a planar Cu_6 hexagon sandwiched between two staggered Cu_3 faces, the Cu_6 ring in $\mathbf{1_H}$ has a nonplanar chair conformation, and one of the two triangular Cu_3 faces is significantly larger than the other (Figure 2b). A view along the C_3 axis (Figure 2c) reveals that these top (smaller) and bottom (larger) triangles of the cuboctahedron are further covered by a Cu_6 cupola and one capping Cu atom, respectively. Within the copper-centered Cu_{13} cuboctahedron, the Cu–Cu distances are in the range 2.5051(4)–2.8281(5) Å, except for the long edges of the bottom triangular face (3.0911(6) Å). Within the Cu_6 capping cupola they are in the range 2.5695(5)–2.7182(4) Å. Except for the longer triangular edges, these values are consistent with the 2.5284(9)–2.8595(7) Å range reported for $\mathbf{1_H}$.[18] The entire copper framework is covered by nine diselenophosphate (dsep) ligands with equal distribution in three spherical rows. Each dsep ligand on both end rows connects an irregular quadrilateral Cu_4 face in a tetrametallic tetraconnective (η^4:μ_2,μ_2) pattern, and those of the middle row bond in a trimetallic tetraconnective (η^3:μ_2,μ_2) pattern to one Cu atom of a Cu_6 unit and two Cu atoms from the chair part of the cuboctahedron (Figure 2d). The Cu–μ_2-Se distances are in the range 2.4208(3)–2.6883(4) Å.[21] Although $\mathbf{2_H}$ and $\mathbf{1_H}$ exhibit the same number of copper–chalcogen bonds (36), the distribution of these bonds over the metal atoms is different. In $\mathbf{1_H}$, all 18 surface copper atoms are each bonded to two sulfur atoms.[18] The 19 surface Cu atoms of $\mathbf{2_H}$ can be classified into seven types of symmetry-related atoms (labeled A–G) in a ratio of 3:3:3:3:3:3:1 (Figure 2c). The B- and G-type atoms are bonded to three Se atoms, the A-, E-, and F-type atoms to two Se atoms, and the C- and D-type atoms to only one Se atom.

The structure of $\mathbf{2_H}$ as determined by neutron diffraction is depicted in Figure 2e. It shows the 11 hydride ligands (grouped into five types of symmetry-related atoms), of which seven (1 + 3 + 3) are capping μ_3-H ligands and four (3 + 1) are in interstitial μ_5-H locations. The three-coordinated (μ_3-H5M) hydride situated on the C_3 axis caps an apical triangle of the Cu_6 cupola, and the remaining six (3 + 3; μ_3-H) hydrides bridge six triangular faces of the cuboctahedron, in alternating up and down positions along the sides of the Cu_6 chair. The average Cu–μ_3-H bond length, 1.70(7) Å, is close to the average distances of 1.71(4) and 1.76(3) Å reported for $\mathbf{1_H}$[18] and $[Cu\{P(p\text{-tolyl})_3\}(\mu_3\text{-H})]_6$,[11a] respectively. One of the five-coordinated interstitial hydrides (μ_5-H1M) is located on the C_3 axis in trigonal-bipyramidal coordination ($\tau = 1.00$).[22] It occupies a cavity generated by the bottom (large) triangular face of the Cu_{12} cuboctahedron, the encapsulated Cu atom, and the bottom capping metal with Cu–H1M distances ranging from 1.7897(12) to 1.920(5) Å. To the best of our knowledge, there has been no previous example of a five-coordinated hydride ligand in a trigonal-bipyramidal coordination site in a homometallic hydride.[23] The other three symmetry-related five-coordinated hydrides (μ_5-H) lie in square-pyramidal cavities[24] ($\tau \approx 0.04$) created by two atoms of the Cu_6 cupola and three atoms of the cuboctahedron. The (Cu–μ_5-H4M) bond distances, 1.675(3)–2.056(3) Å, are comparable with those [1.774(9)–2.121(8) Å] identified by single-

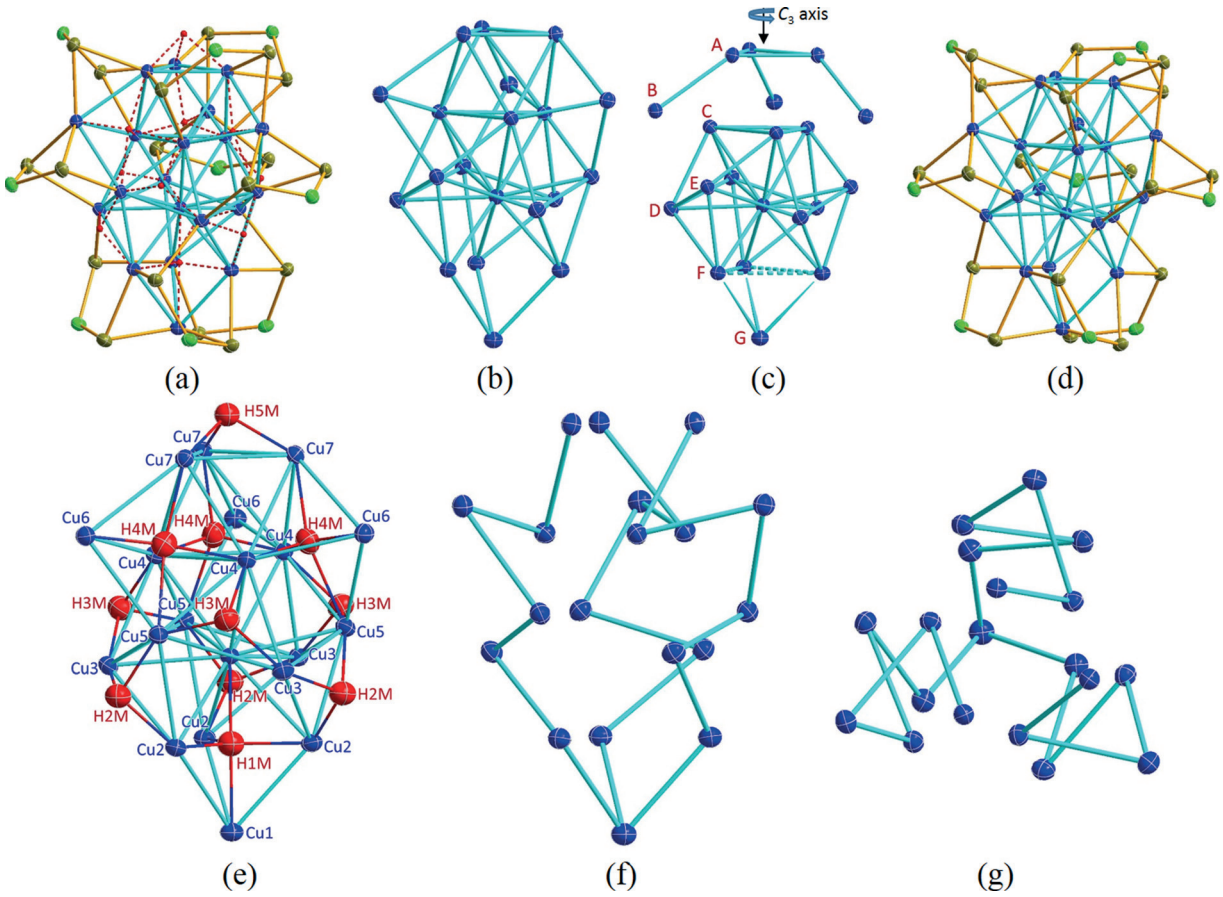

Figure 2. a) Full molecular structure of $\mathbf{2_H}$ (isopropoxy groups have been omitted for clarity). b) Complete Cu_{20} framework. c) Fragmentation of the Cu_{20} core by the labeling of different surface-atom types (A–G): The central cuboctahedron Cu_{13} (C–F) combines with a Cu_6 (A,B) cupola and a single Cu atom (G). d) Cu_{20} core shielded by nine $[Se_2P(OiPr)_2]^-$ ligands with equal distribution in three spherical rows. e) Structure of the $Cu_{20}H_{11}$ moiety with the five types of symmetry-related hydride ligands, as determined by neutron diffraction. f,g) Side and top views of the three anticlockwise copper strands constituting the Cu_{20} core. Color code: Cu blue, Cu–Cu edges cyan, Se yellow, P green, H red.

crystal neutron diffraction in $[Cu_{32}H_{20}\{S_2P(OiPr)_2\}_{12}]$.[20] On the basis of the structural description mentioned above, a peculiar bonding situation of the central copper atom, Cu8, arises. Apart from its 12 Cu–Cu (d^{10}–d^{10}) contacts, it is bonded to only one hydride. The coordination environments of the other copper types are SeH_3 ($Cu_{C,D}$), Se_2H_2 ($Cu_{A,E,F}$), and Se_3H ($Cu_{B,G}$).

The Cu_{20} chiral core of $\mathbf{2_H}$ represents an unprecedented arrangement of copper atoms, as shown by a side view in Figure 2c, in which the 19 surface Cu atoms can be classified into seven types of symmetry-related atoms (A–G) in a ratio of 3:3:3:3:3:3:1. Three groups of every single Cu atom type create three anticlockwise helices along the C_3 axis (Figure 2f,g). To the best of our knowledge, no structural evidence of a nanoscale, hydrido metal cluster with an intrinsic chiral metallic core has been presented previously. This structural feature is similar to that of a recently discovered thiol-stabilized gold cluster, in which an Au_{20} core of C_3 symmetry had an intrinsically chiral inorganic core.[25] Unfortunately, $\mathbf{2_H}$ crystallizes in the central symmetric space group $R\bar{3}$, so that no optical activity is revealed in its CD spectrum.

In agreement with the structure determined by neutron diffraction, the $^{31}P\{^1H\}$ NMR spectrum of $\mathbf{2_H}$ at ambient temperature displays three resonances of equal intensity at 98.6 ($^1J_{Se,P} = 691.3$, 637.8 Hz), 89.6 (674.9, 616.0 Hz), and 54.0 ppm (598.9 Hz; see Figure S3). The broad selenium satellite of the phosphorus peak at 54.0 ppm was well resolved into the expected double doublet pattern when the temperature was decreased (see Figure S4). These results indicate that there are three types of dsep ligand, and both selenium atoms of each dsep ligand type are chemically inequivalent. Thus, there exist six types of selenium atoms in the molecule, as also supported by the $^{77}Se\{^1H\}$ NMR spectrum with the appearance of six doublet resonances centered at 192.48 ($^1J_{Se,P} = 644.5$ Hz), 49.04 (672.7 Hz), −8.38 (703.6 Hz), −35.60 (566.0 Hz), −102.15 (609.6 Hz), and −144.77 (640.8 Hz; see Figure S5). These splitting patterns can be attributed to the asymmetric arrangement of the copper atoms, and their binding to both selenium atoms of each dsep ligand result in two chemically and magnetically non-equivalent selenium atoms within each dsep ligand type. Overall, these NMR spectroscopic results support the intrinsic chirality of the Cu_{20} core of $\mathbf{2_H}$ in solution. As a result of this intrinsic chirality, the $^1H/^2H$ NMR spectrum of the hydride in $\mathbf{2_H}$ and the deuteride in $[Cu_{20}D_{11}\{Se_2P(OiPr)_2\}_9]$ ($\mathbf{2_D}$) should display five types of hydride resonances in a ratio of 1:3:3:3:1 (Figure 2e). Experimentally, five broad singlet deuteride resonances at

−1.28, −0.63, −0.52, 3.01, and 3.27 ppm with an integral ratio of 3:3:1:1:3 were observed in the ^{2}H NMR spectrum of $\mathbf{2_D}$ (see Figure S6A). These signals are absent in its ^{1}H NMR spectrum (see Figure S6B). On the other hand, the ^{1}H NMR spectrum of $\mathbf{2_H}$ (see Figure S6C) displays three broad hydride peaks at −1.31, −0.65, and 3.11 ppm in a ratio of 3:(3+1):(1+3). The expected splitting of each of the hydride peaks at −0.65 and 3.11 ppm into two peaks in a 3:1 ratio was not observed until the temperature was lowered to −90 °C (see Figure S7A,B). Thus, the observed pattern of hydride resonances is consistent with the location of the hydride ligands in the neutron single-crystal structure and also strongly reflects the existence of five types of hydride ligand in $\mathbf{2_H}$ owing to the C_3 arrangement of Cu atoms. Once again, the intrinsic chirality of the Cu_{20} core is well demonstrated. The UV/Vis absorption spectrum of $\mathbf{2_H}$ in solution displays a band at around 386 nm along with two broad bands at 455 and 511 nm (see Figure S8).

The DFT-optimized geometry of the $\mathbf{2'_H}$ model led to a structure with very close to C_3 symmetry that is fully consistent with the experimental structural data (Table 1).

Table 1: Selected metric parameters and ^{1}H NMR hydride shifts for $\mathbf{2_H}$ and the corresponding DFT-computed values.

	Bond lengths [Å][a]	^{1}H NMR chemical shifts	
		experimental ($CDCl_3$)	calculated
Cu_{cup}–μ_3-H[b]	1.730(3) {1.735–1.738}	−0.52	−0.25
Cu_{cubo}–μ_3-H[b]	1.680(3)–1.723(3) {1.680–1.755}	−1.28, −0.63	0.74, −0.10
Cu–μ_5-H_{sp}[b]	1.675(3)–2.056(3) {1.686–2.042}	3.27	3.74
Cu–μ_5-H_{tbp}[b]	1.7897(12)–1.920(5) {1.790–1.934}	3.01	3.64
Cu_{cent}–Cu_{cubo}[b]	2.5859(4)–2.7213(5) {2.596–2.760}	–	–
$[Cu–Cu]_{cubo}$[b]	2.5051(4)–2.8281(5) {2.592–2.697}	–	
Cu_{cubo}–Cu_{cup}[b]	2.5809(4)–2.7793(4) {2.585–2.770}	–	–
Cu_{cubo}–Cu_{cap}[b]	2.6209(5) {2.637–2.643}	–	–

[a] Cu–Cu bond lengths were determined by X-ray diffraction; Cu–H bond lengths were determined by neutron diffraction. The values in curly brackets are the theoretical bond lengths from DFT calculations. [b] cup = cupola, cubo = cuboctahedron, sp = square pyramid, tbp = trigonal bipyramid, cent = center, cap = capping.

Moreover, there is reasonably good consistency between the computed and observed hydride NMR chemical shifts, as exemplified by the linear correlation that exists between the two sets of values (see Figure S9). The hydride natural orbital charges are between −0.60 and −0.45, whereby the encapsulated hydride ligands are more negatively charged than the outer μ_3-H atoms. These charges are indicative of significant covalency. The Cu–Cu Wiberg indices of the Cu_{19} cage lie in the usual range (0.04–0.08) found for weak d^{10}–d^{10} interactions of this type.[18–20] The values associated with the encapsulated metal, Cu8, are somewhat larger (0.08–0.12) and indicate weak covalent interactions resulting from electron donation from filled 3d orbitals of the Cu cage into the 4s/4p orbitals of the encapsulated metal. This effect is evidenced by the valence electron configuration of this encapsulated atom ($3d^{9.91}\ 4s^{0.92}\ 4p^{0.28}$) as compared to the averaged configuration of the copper atoms that constitute the Cu_{19} cage ($3d^{9.83}\ 4s^{0.52}\ 4p^{0.03}$). The atomic charges of these cage atoms range between +0.45 and +0.60, whereas a negative charge of −0.12 on the encapsulated metal arises from this covalent interaction, which is the major stabilizing component governing the existence of the encapsulated (formally Cu^I) atom, which is bonded to only one hydride ligand (see above). Thus, the 12-fold "d^{10}–d^{10}" interactions in the center cuboctahedron build up some electron density within this volume. This electron density is to some extent responsible for the cohesion of the structure, in the same way (but to a lesser degree) as jellium-type electrons are in superatom-like clusters.[26]

We also investigated the stability of the chiral $\mathbf{2'_H}$ structure with respect to that of its hypothetical C_{3h} "isomer" by calculations on the selenium analogue of $\mathbf{1_H}$, namely, $[Cu_{20}H_{11}\{Se_2PH_2\}_9]$ ($\mathbf{1''_H}$). Consistent with experiment, $\mathbf{2'_H}$ was found to be more stable than $\mathbf{1''_H}$ by 19 kcal mol^{-1}.

In summary, chalcogen-ligand exchange on the symmetrical nanocluster $[Cu_{20}H_{11}\{S_2P(OiPr)_2\}_9]$ ($\mathbf{1_H}$) induced the formation of the asymmetric nanocluster $[Cu_{20}H_{11}\{Se_2P(OiPr)_2\}_9]$ ($\mathbf{2_H}$), which exhibits an intrinsically chiral Cu core in both solution and solid states. No metal hydride cluster with a chiral core has been reported previously. Unlike its sulfur analogue,[18] the nanospheric cluster $\mathbf{2_H}$ features a distorted central Cu_{13} cuboctahedron with, along this symmetry axis, an additional Cu_6 cupola staple motif on one side and a single capping Cu atom on the other side. Among the various coordination modes of capping (μ_3-H) and interstitial hydrides (μ_5-H) in $\mathbf{2_H}$, a five-coordinated H atom in a trigonal-bipyramidal location was observed for the first time in a homometallic hydride cluster.[23] DFT calculations confirmed the stability of the $\mathbf{2_H}$ architecture and brought to light the generation of 4s/4p electron density in the center of the cuboctahedron; this electron density is responsible for the stability of the cuboctahedron. The insight obtained into the chirality of cluster $\mathbf{2_H}$ could offer new perspectives for stereoselective reactions, such as the reduction of unsaturated hydrocarbons.[14]

Acknowledgements

This research was supported by the Ministry of Science and Technology of Taiwan (MOST 103-2113-M-259-003, 103-2739-M-213-001-MY3). Studies performed with the TOPAZ instrument of the ORNL Spallation Neutron Source were sponsored by the Scientific User Facilities Division, Office of Basic Energy Sciences, US Department of Energy. CCDC 1411898 ($\mathbf{2_H}$, X-ray), 1411337 ($\mathbf{2_H}$, neutron) contain the supplementary crystallographic data for this paper. These data can be obtained free of charge from The Cambridge Crystallographic Data Centre.

Keywords: copper · density functional calculations · hydrides · intrinsic chirality · neutron diffraction

How to cite: *Angew. Chem. Int. Ed.* **2015**, *54*, 13604–13608
Angew. Chem. **2015**, *127*, 13808–13812

[1] a) L. O. Brown, J. E. Hutchison, *J. Am. Chem. Soc.* **1999**, *121*, 882; b) Y. Shichibu, Y. Negishi, T. Tsukuda, T. Teranishi, *J. Am. Chem. Soc.* **2005**, *127*, 13464; c) F. Dubois, B. Mahler, B. Dubertret, E. Doris, C. Mioskowski, *J. Am. Chem. Soc.* **2007**, *129*, 482; d) C. A. Fields-Zinna, J. F. Parker, R. W. Murray, *J. Am. Chem. Soc.* **2010**, *132*, 17193; e) V. R. Jupally, R. Kota, E. V. Dornshuld, D. L. Mattern, G. S. Tschumper, D.-e. Jiang, A. Dass, *J. Am. Chem. Soc.* **2011**, *133*, 20258; f) D. Ling, M. J. Hackett, T. Hyeon, *Nano Today* **2014**, *9*, 457.

[2] a) C. Mirkin, R. Letsinger, R. Mucic, J. Storhoff, *Nature* **1996**, *382*, 607; b) P. Mulvaney, *Langmuir* **1996**, *12*, 788; c) J. Hicks, A. Templeton, S. Chen, K. Sheran, R. Jasti, R. Murray, J. Debord, T. Schaaff, R. Whetten, *Anal. Chem.* **1999**, *71*, 3703; d) G. Konstantatos, I. Howard, A. Fischer, S. Hoogland, J. Clifford, E. Klem, L. Levina, E. H. Sargent, *Nature* **2006**, *442*, 180.

[3] a) C. L. Heinecke, T. W. Ni, S. Malola, V. Mäkinen, O. A. Wong, H. Häkkinen, C. J. Ackerson, *J. Am. Chem. Soc.* **2012**, *134*, 13316; b) T. W. Ni, M. A. Tofanelli, B. D. Phillips, C. J. Ackerson, *Inorg. Chem.* **2014**, *53*, 6500.

[4] C. Zeng, C. Liu, Y. Pei, R. Jin, *ACS Nano* **2013**, *7*, 6138.

[5] a) X. Meng, Q. Xu, S. Wang, M. Zhu, *Nanoscale* **2012**, *4*, 4161; b) Q. Xu, S. Wang, Z. Liu, G. Xu, X. Meng, M. Zhu, *Nanoscale* **2013**, *5*, 1176; c) W. Kurashige, M. Yamaguchi, K. Nobusada, Y. Negishi, *J. Phys. Chem. Lett.* **2012**, *3*, 2649; d) W. Kurashige, S. Yamazoe, K. Kanehira, T. Tsukuda, Y. Negishi, *J. Phys. Chem. Lett.* **2013**, *4*, 3181.

[6] a) A. J. Hoskin, D. W. Stephan, *Coord. Chem. Rev.* **2002**, *233*, 107; b) M. Konkol, J. Okuda, *Coord. Chem. Rev.* **2008**, *252*, 1577.

[7] a) M. A. Esteruelas, L. A. Oro, *Chem. Rev.* **1998**, *98*, 577; b) S. Gaillard, J.-L. Renaud, *ChemSusChem* **2008**, *1*, 505.

[8] a) *Catalysis by Di- and Polynuclear Metal Cluster Complexes* (Eds.: R. D. Adams, F. A. Cotton), Wiley-VCH, New York, **1998**; b) H. Suzuki, *Eur. J. Inorg. Chem.* **2002**, 1009.

[9] a) J. Graetz, *Chem. Soc. Rev.* **2009**, *38*, 73; b) J. Yang, A. Sudik, C. Wolvertonb, D. J Siegelwa, *Chem. Soc. Rev.* **2010**, *39*, 656; c) M. Ephritikhine, *Chem. Rev.* **1997**, *97*, 2193; d) Z. Hou, M. Nishiura, T. Shima, *Eur. J. Inorg. Chem.* **2007**, 2535; e) G. J. Kubas, *Chem. Rev.* **2007**, *107*, 4152; f) M. Takimoto, Z. Hou, *Nature* **2006**, *443*, 400.

[10] a) A. Wurtz, *Ann. Chim. Phys.* **1844**, *11*, 250; b) A. Wurtz, *C. R. Hebd. Seances Acad. Sci.* **1844**, *18*, 702.

[11] a) R. C. Stevens, M. R. McLean, R. Bau, T. F. Koetzle, *J. Am. Chem. Soc.* **1989**, *111*, 3472; b) W. S. Mahoney, D. M. Brestensky, J. M. Stryker, *J. Am. Chem. Soc.* **1988**, *110*, 291.

[12] H. Lv, Y.-B. Cai, J.-L. Zhang, *Angew. Chem. Int. Ed.* **2013**, *52*, 3203; *Angew. Chem.* **2013**, *125*, 3285.

[13] a) C. Deutsch, N. Krause, B. H. Lipshutz, *Chem. Rev.* **2008**, *108*, 2916; b) "Copper(I) Hydride Reagents and Catalysts": O. Riant in *Chemistry of Functional Groups* (Ed.: S. Patai), Wiley, Hoboken, **2011**.

[14] a) R. Moser, Ž. V. Bošković, C. S. Crowe, B. H. Lipshutz, *J. Am. Chem. Soc.* **2010**, *132*, 7852; b) A. V. Malkov, *Angew. Chem. Int. Ed.* **2010**, *49*, 9814; *Angew. Chem.* **2010**, *122*, 10008; c) B. H. Lipshutz in *Copper-Catalyzed Asymmetric Synthesis* (Eds. A. Alexakis, N. Krause, S. Woodward), Wiley-VCH, Weinheim, **2014**, chap. 7, p. 179.

[15] a) S.-L. Shi, S. L. Buchwald, *Nat. Chem.* **2015**, *7*, 38; b) E. Ascic, S. L. Buchwald, *J. Am. Chem. Soc.* **2015**, *137*, 4666; c) S. Zhu, S. L. Buchwald, *J. Am. Chem. Soc.* **2014**, *136*, 15913; d) Y. Miki, K. Hirano, T. Satoh, M. Miura, *Angew. Chem. Int. Ed.* **2013**, *52*, 10830; *Angew. Chem.* **2013**, *125*, 11030.

[16] a) M. S. Eberhart, J. R. Norton, A. Zuzek, W. Sattler, S. Ruccolo, *J. Am. Chem. Soc.* **2013**, *135*, 17262; b) C. M. Wyss, B. K. Tate, J. Bacsa, T. G. Gray, J. P. Sadighi, *Angew. Chem. Int. Ed.* **2013**, *52*, 12920; *Angew. Chem.* **2013**, *125*, 13158; c) M. A. Huertos, I. Cano, N. A. G. Bandeira, J. Benet-Buchholz, C. Bo, P. W. N. M. V. Leeuwen, *Chem. Eur. J.* **2014**, *20*, 16121; d) K. Nakamae, B. Kure, T. Nakajima, Y. Ura, T. Tanase, *Chem. Asian J.* **2014**, *9*, 3106; e) C. Ganesamoorthy, J. Weßing, C. Kroll, R. W. Seidel, C. Gemel, R. A. Fischer, *Angew. Chem. Int. Ed.* **2014**, *53*, 7943; *Angew. Chem.* **2014**, *126*, 8077; f) T.-A. D. Nguyen, B. R. Goldsmith, H. T. Zaman, G. Wu, B. Peters, T. W. Hayton, *Chem. Eur. J.* **2015**, *21*, 5341; g) E. L. Bennett, P. J. Murphy, S. Imberti, S. F. Parker, *Inorg. Chem.* **2014**, *53*, 2963.

[17] a) C. W. Liu, B. Sarkar, Y.-J. Huang, P.-K. Liao, J.-C. Wang, J.-Y. Saillard, S. Kahal, *J. Am. Chem. Soc.* **2009**, *131*, 11222; b) P.-K. Liao, B. Sarkar, H.-W. Chang, J.-C. Wang, C. W. Liu, *Inorg. Chem.* **2009**, *48*, 4089; c) P.-K. Liao, K.-G. Liu, C.-S. Fang, C. W. Liu, J. P. Fackler, Y.-Y. Wu, *Inorg. Chem.* **2011**, *50*, 8410; d) P.-K. Liao, C.-S. Fang, A. J. Edwards, S. Kahlal, J.-Y. Saillard, C. W. Liu, *Inorg. Chem.* **2012**, *51*, 6577; e) P.-K. Liao, D.-R. Shi, J.-H. Liao, C. W. Liu, A. V. Artemev, V. A. Kuimov, N. K. Gusarova, B. A. Trofimov, *Eur. J. Inorg. Chem.* **2012**, 4921; f) C. Latouche, S. Kahlal, Y.-R. Lin, J.-H. Liao, E. Furet, C. W. Liu, J.-Y. Saillard, *Inorg. Chem.* **2013**, *52*, 13253; g) C. Latouche, S. Kahlal, E. Furet, P.-K. Liao, Y.-R. Lin, C.-S. Fang, J. Cuny, C. W. Liu, J.-Y. Saillard, *Inorg. Chem.* **2013**, *52*, 7752; h) C. Latouche, C. W. Liu, J.-Y. Saillard, *J. Cluster Sci.* **2014**, *25*, 147.

[18] a) R. S. Dhayal, J.-H. Liao, Y.-R. Lin, P.-K. Liao, S. Kahlal, J.-Y. Saillard, C. W. Liu, *J. Am. Chem. Soc.* **2013**, *135*, 4704; b) J.-H. Liao, R. S. Dhayal, X. Wang, S. Kahlal, J.-Y. Saillard, C. W. Liu, *Inorg. Chem.* **2014**, *53*, 11140.

[19] A. J. Edwards, R. S. Dhayal, P.-K. Liao, J.-H. Liao, M.-H. Chiang, R. O. Piltz, S. Kahlal, J.-Y. Saillard, C. W. Liu, *Angew. Chem. Int. Ed.* **2014**, *53*, 7214; *Angew. Chem.* **2014**, *126*, 7342.

[20] R. S. Dhayal, J.-H. Liao, S. Kahlal, X. Wang, Y.-C. Liu, M.-H. Chiang, W. E. van Zyl, J.-Y. Saillard, C. W. Liu, *Chem. Eur. J.* **2015**, *21*, 8369.

[21] T. S. Lobana, J.-C. Wang, C. W. Liu, *Coord. Chem. Rev.* **2007**, *251*, 91.

[22] For a definition of the angular geometric parameter (τ), see: A. W. Addison, T. N. Rao, J. Reedijk, J. van Rijin, G. C. Verschoor, *J. Chem. Soc. Dalton Trans.* **1984**, 1349.

[23] For examples of heteroleptic μ_5-H ligands with tbp coordination geometry, as identified by neutron diffraction, see: a) T. Shima, Y. Luo, T. Stewart, R. Bau, G. J. McIntyre, S. A. Mason, Z. Hou, *Nat. Chem.* **2011**, *3*, 814; b) T. U. Blankenship, X. Wang, C. Hoffmann, S. E. Latturner, *Inorg. Chem.* **2014**, *53*, 10620.

[24] R. Bau, M. H. Drabnis, L. Garlaschelli, W. T. Klooster, Z. Xie, T. F. Koetzle, S. Martinengo, *Science* **1997**, *275*, 1099.

[25] X.-K. Wan, S.-F. Yuan, Z.-W. Lin, Q.-M. Wang, *Angew. Chem. Int. Ed.* **2014**, *53*, 2923; *Angew. Chem.* **2014**, *126*, 2967.

[26] M. Walter, J. Akola, O. Lopez-Acevedo, P. D. Jadzinsky, G. Calero, C. J. Ackerson, R. L. Whetten, H. Grönbeck, H. Häkkinen, *Proc. Natl. Acad. Sci. USA* **2008**, *105*, 9157.

Received: July 21, 2015
Published online: September 21, 2015

